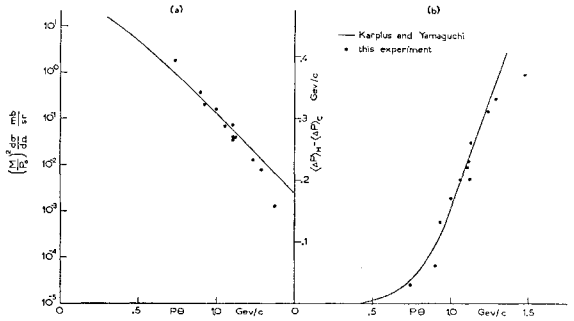

FIG. 2. Comparison between the results of this experiment and calculations of Karplus and Yamaguchi[4] on plural quasi-elastic scattering. (a) compares the laboratory differential cross sections, and (b) the separation between the laboratory momentum of the peak from p-C scattering and that of p-p elastic scattering.

transfer is about 1 Gev/c. The result is two peaks, one from single scattering at the same momentum as for elastic p-p scattering and the other, from double scattering, at half the momentum loss. These two peaks are broadened by the fermi motion and, in general, merge into a single peak. The spectrum at 26.02 Gev/c, where the highest momentum transfer is involved, shows the two peaks resolved.

Figure 2 shows a comparison between the experimental results and the calculations of Karplus and Yamaguchi; Fig. 2(b) compares the values of $\langle\Delta P\rangle_H - \langle\Delta P\rangle_C$, and Fig. 2(a) shows the p-C differential cross section as a function of the momentum transfer. The agreement is good.

Figure 1(d) shows the momentum spectra for p-d and p-p scattering. The p-d spectrum shows two clearly resolved peaks, one at the same momentum as the elastic p-p peak, the other at half the momentum loss. There are two obvious possible explanations of the higher momentum peak, double quasi-elastic scattering, and single coherent scattering from the deuteron as a whole. The latter seems unlikely as the momentum transfer (1.1 Gev/c) is large compared to the deuteron binding energy.

We should like to thank Dr. R. Karplus and Dr. Y. Yamaguchi for stimulating discussions and L. Bird, R. Donnet, and C. A. Ståhlbrandt for their continuous assistance.

PHYSICAL REVIEW VOLUME 126, NUMBER 1 APRIL 1, 1962

π^-–p Interactions at 1.3 Bev*†

W. D. SHEPHARD‡§ AND W. D. WALKER
University of Wisconsin, Madison, Wisconsin

(Received October 9, 1961)

A study has been made of the interactions of 1.3-Bev π^- mesons from the Cosmotron in the Columbia 12-in. propane bubble chamber. Out of a total of 1401 two-prong interactions measured and analyzed, 587 were classified as hydrogen interactions. Techniques used in scanning, measurement, and analysis, and the uncertainties involved in these techniques are discussed with special reference to the problem of carbon contamination. Corrections to the data are calculated. Best values for cross sections at this energy are: $\sigma_{el}=10.5\pm0.8$ mb, $\sigma_{\pi^-\pi^+n}=9.2\pm1.4$ mb, $\sigma_{\pi^-\pi^0p}=6.2\pm0.9$ mb, $\sigma_{neutral}=5.2\pm0.2$ mb, and $\sigma_{\pi^-\pi^-\pi^+p}=1.0_{-0.3}{}^{+0.5}$ mb, normalized to $\sigma_{total}=34.7\pm1.2$ mb. A study of $\pi^-+n\rightarrow\pi^-+\pi^-+p$ events in carbon is used to provide evidence on carbon contamination in single pion production. The data on single pion production processes are compared in detail with the predictions of the statistical model, the isobar model, and pion-pion interaction theory. The extended isobar model gives qualitative agreement with some features of the c.m. momentum spectra, but quantitative agreement is poor. Evidence is found for a resonance in $\sigma_{\pi\pi}(\omega)$ between 700 and 800 Mev total energy for the dipion system. The data are consistent with a resonance in the $T=J=1$ $\pi-\pi$ state. A rise in the $\pi-\pi$ cross section at low energies appears to occur. Differences in results for (π^-,π^+,n) and (π^-,π^0,p) events are considered. Evidence for final-state pion-nucleon interactions in conjunction with pion-pion interactions is presented.

I. INTRODUCTION

AT the present time there is considerable interest in the interactions of pions with nucleons at energies in the Bev region. Total and elastic cross sections have been measured in detail in several experiments for energies ranging from a few hundred Mev to about 1.5 Bev.[1–7] A summary of many of the

* Supported in part by the U. S. Atomic Energy Commission and in part by the Research Committee of the University of Wisconsin with funds provided by Wisconsin Alumni Research Foundation.

† This work has been submitted by W. D. Shephard to the University of Wisconsin in partial fulfillment of the requirements for the degree of Doctor of Philosophy.

‡ Present address: Physics Department, University of Kentucky, Lexington, Kentucky.

§ Supported in part during latter stages of the work by National Science Foundation.

[1] T. J. Devlin, B. C. Barish, W. N. Hess, V. Perez-Mendez, and J. Solomon, Phys. Rev. Letters **4**, 242 (1960).
[2] J. C. Brisson, J. T. Detouf, P. Falk-Vairant, L. Van Rossum, and G. Valladas, Nuovo cimento **19**, 210 (1961).
[3] J. I. Shonle, Phys. Rev. Letters **5**, 156 (1960).
[4] W. D. Walker, F. Hushfar, and W. D. Shephard, Phys. Rev. **104**, 526 (1956).
[5] M. Chretien, J. Leitner, N. P. Samios, M. Schwartz, and J. Steinberger, Phys. Rev. **108**, 383 (1957).
[6] L. M. Eisberg, W. B. Fowler, R. M. Lea, W. D. Shephard, R. P. Shutt, A. M. Thorndike, and W. L. Whittemore, Phys. Rev. **97**, 797 (1955).
[7] W. D. Walker and J. Crussard, Phys. Rev. **98**, 1416 (1955).

measurements up until early 1960 will be found in the article on cross sections by Brisson *et al.*[2]

Interest in pion production in $\pi - p$ collisions has increased with the development of models for comparison with experiment, including the Lindenbaum-Sternheimer isobaric nucleon model[8–12] and various pion-pion interaction theories.[13–16] Several pion production studies near 1 Bev have been made and comparisons with the models have been published.[15,17–24] Preliminary results of pion production by[16] 1.89-Bev/c π^- and by π^+ at several energies[25] are available.

A study of 1.3-Bev π^- interactions in the Columbia University 12-in. propane bubble chamber at the Brookhaven Cosmotron is reported here. Studies of strange particle production[26,27] and elastic scattering[5,28] at this energy in this and related exposures have been published. In this experiment the final states considered in detail are (π^-,π^+,n) and (π^-,π^0,p). Some information on elastic scattering, multiple pion production, and $\pi^- - C$ interactions has been obtained.

II. EXPERIMENTAL PROCEDURE

The physical dimensions and operating characteristics of the bubble chamber used in this experiment have been published in reports of the strange particle production in this exposure.[26] The chamber was a cylinder of aluminum with an inside diameter of 12 in. and a depth of 8 in. It was filled with liquid propane (C_3H_8) at a temperature of 57°C. The density of the expanded propane was 0.429 ± 0.010 g/cm^2. The chamber was operated in a magnetic field with nominal value of 13.4 kgauss. Pictures of the chamber were taken with 3 cameras located 120° apart on the circumference of a $11\frac{1}{2}$-in. diameter circle 40 in. from the inside of the chamber window and parallel to it. Fiducial marks on the insides of the windows provide reference marks for measurements on the pictures.

The chamber was operated in a negative pion beam with a mean momentum of 1.433 ± 0.015 Bev/c. The details of the beam have been published elsewhere.[5,26–28] The absolute value of the beam momentum was obtained from a study of two strange-particle production events, and the spread in beam energy was calculated from trajectories plotted through the collimation system.[27,28] In the calculations of this experiment an incoming pion momentum of 1.44 Bev/c was assumed.

A total of 18 000 pictures were taken in the exposure of which approximately 3500 pictures were examined in this experiment. The number of beam tracks varied widely about an average of approximately 12 tracks per picture.

Scanning and measuring were both performed on a projector with an optical system similar to that with which the pictures were taken. The size of the projected image was approximately twice the size of the chamber, and all three views of the chamber were projected. Measurements of coordinates and angles were made with a drafting engine. Coordinates were measured to the nearest 0.5 mm and angles to the nearest 0.1° on the projections. Curvatures were measured with templates.

In the initial scanning all measurable $(-+)$ and $(--++)$ events were measured. In a second scanning of a fiducial region defined by a rectangle in one of the projections all events were classified by appearance as: (1) $(-+)$ star; (2) $(--++)$ star; (3) track ending; (4) deflection; (5) $(--+)$ star; or (6) other stars.

No events in the fiducial region should escape detection and few should fail to satisfy measurement criteria. The $(--+)$ events and track endings were measured during the second scan and the number of beam tracks through the region was recorded for every fifth picture. In approximately 20% of the pictures the scanning of the fiducial region was repeated by a different observer to obtain data for calculation of scanning efficiencies.

Criteria for event measurement were: (1) the vertex must be clearly visible and show secondaries of the proper numbers and charges; (2) the primary must be of measurable length and consistent in direction and curvature with the beam; and (3) all secondaries must have projected lengths $\geqslant 10$ cm in all views.

Measurements on all 3 projected views were made and other features such as bubble density were noted where they might be of use. A total of 1401 $(-+)$

[8] S. J. Lindenbaum and R. M. Sternheimer, Phys. Rev. **105**, 1874 (1957).
[9] S. J. Lindenbaum and R. M. Sternheimer, Phys. Rev. **106**, 1107 (1957).
[10] S. J. Lindenbaum and R. M. Sternheimer, Phys. Rev. **109**, 1723 (1958).
[11] S. J. Lindenbaum and R. M. Sternheimer, Phys. Rev. Letters **5**, 24 (1960).
[12] R. M. Sternheimer and S. J. Lindenbaum, Phys. Rev. **123**, 333 (1961).
[13] C. Goebel, Phys. Rev. Letters **1**, 337 (1958).
[14] G. F. Chew and F. E. Low, Phys. Rev. **113**, 1640 (1959).
[15] F. Bonsignori and F. Selleri, Nuovo cimento **15**, 465 (1960).
[16] A. R. Erwin, R. March, W. D. Walker, and E. West, Phys. Rev. Letters **6**, 628 (1961).
[17] L. Baggett, Jr., thesis, University of California Radiation Laboratory Report UCRL-8302, 1958 (unpublished).
[18] V. Alles-Borelli, S. Bergia, E. Perez-Ferreira, and P. Waloschek, Nuovo cimento **14**, 211 (1959).
[19] I. Derado and N. Schmitz, Phys. Rev. **118**, 309 (1960).
[20] I. Derado, Nuovo cimento **15**, 853 (1960).
[21] V. P. Kenney, University of Kentucky (private communication).
[22] E. Pickup, F. Ayer, and E. O. Salant, Phys. Rev. Letters **5**, 161 (1960).
[23] J. G. Rushbrook and D. Radojicic, Phys. Rev. Letters **5**, 567 (1960).
[24] B. A. Munir, E. Pickup, D. K. Robinson, and E. O. Salant, Phys. Rev. Letters **6**, 192 (1961).
[25] D. Stonehill, C. Baltay, H. Courant, W. Fickinger, E. C. Fowler, H. Kraybill, J. Sandweiss, J. Sanford, and H. Taft, Phys. Rev. Letters **6**, 624 (1961).
[26] F. Eisler, R. Plano, A. Prodell, N. Samios, M. Schwartz, J. Steinberger, P. Bassi, V. Borelli, G. Puppi, H. Tanaka, P. Waloschek, V. Zoboli, M. Conversi, P. Franzini, I. Manelli, R. Santangelo, and V. Silvestrini, Nuovo cimento **10**, 468 (1958).
[27] R. Budde, M. Chretien, J. Leitner, N. Samios, M. Schwartz, and J. Steinberger, Phys. Rev. **103**, 1827 (1956).
[28] J. Leitner, Columbia University Report NEVIS-28, 1957 (unpublished).

events were measured of which 1092 were in the fiducial region.

Conversion from measurements to space coordinates, angles, and momenta was made with an IBM 650 computer. Calculations were performed for each pair of views and the mean values and probable errors were computed. In cases where one pair of views gave poor determinations (all beam tracks plus a few others) only the other pairs were used for calculations. Ranges for stopping particles were calculated.

The probable errors for vertex coordinates were generally 1 to 2 mm in a plane perpendicular to the optic axes of the cameras and about 5–6 mm parallel to the optic axes. Probable errors for the polar angles of tracks were generally 0.5° or less and errors for the azimuthal angles about an axis in approximately the mean beam direction were commonly 3° or less. If significantly larger errors were encountered their cause was sought and corrections made. Events were remeasured and recalculated where necessary. Further details on measurements and calculations are given in reference 29.

III. IDENTIFICATION OF INTERACTIONS

A. Identification Techniques

Kinematic analysis was used to separate interactions in hydrogen and in carbon and to separate different types of interactions in hydrogen. Some types of carbon interactions were clearly identifiable, but no types of hydrogen events could be uniquely identified by appearance.

The first category of events considered was that of $(-+)$ stars. These could be elastic scatterings, single pion productions, or multiple pion productions involving either free protons or bound protons. The incoming momentum was always assumed to be 1.44 Bev/c.

In attempting to separate hydrogen and carbon interactions, the assumption was made that the Fermi momentum of the protons in carbon would be large enough to allow detection of a net energy-momentum imbalance with the measurement accuracy of this experiment. Rather stringent limits on allowed variations of momenta and angles were used in fitting events to reactions in order to eliminate most carbon events. Rejection of some good hydrogen events is expected as a result. This can be estimated from the cross sections measured in other experiments. Some residual carbon contamination is expected and is estimated from examination of $(--+)$ carbon events. Hydrogen events with more than one neutral secondary cannot be separated from carbon events.

Elastic hydrogen interactions were first selected. Coplanarity, angles, and momenta were all used in this selection. A total of 150 elastic events were selected, with 116 in the fiducial region.

The remaining events were then analyzed to see if they were consistent with criteria for (1) $\pi^-+p\rightarrow\pi^-+\pi^++n$, or (2) $\pi^-+p\rightarrow\pi^-+\pi^0+p$ hydrogen events. From conservation of momentum and energy the mass of the assumed neutral secondary was calculated using the computer. All calculations were performed in the laboratory coordinate system to avoid problems in error calculation. An iterative procedure was used with the input angles and momenta varied within uncertainties in an attempt to fit the neutral mass for the assumed interaction. Information from scanning about the nature of the positive secondary was used when available. The criterion for acceptance as a hydrogen event was a neutral mass of 939.5 ± 20 Mev/c^2 for (1) or 135 ± 10 Mev/c^2 for (2). The limits on possible neutral mass for an event were calculated in the first iterations. For almost all acceptable cases, the desired neutral mass lay well within these limits. Hence, the exact mass ranges allowed by the acceptance criterion had little effect on the event classification. They were chosen large enough so that few iterations were needed to obtain acceptable values, but small enough so no significant errors in momenta and angles were expected from the fitting process. Adjustments to the input data were made in approximate proportion to the estimated experimental errors on the input quantities to further limit distortions due to the fitting process.

A similar analysis was performed on the $(--+)$ events to obtain information on the kinematics of carbon events for estimating carbon contamination in the $(-+)$ events. Kinematic analysis of $(--++)$ events was performed to select hydrogen events for cross-section determination.

B. Errors in Identification

Errors in determinations of angles and positions should not significantly affect the selection of events in this experiment. Typical uncertainties have been previously mentioned. Use of three separate determinations for each quantity allows the detection of large errors and the estimation of uncertainties. No significant systematic errors in angles or positions are known. A slight systematic distortion of about 3% in calculated depth of points was present but resultant angular distortions appear insignificant in most cases.

The accuracy of the momentum measurements is the main limitation on event identification in this experiment. The main source of uncertainty in the momentum measurements comes from multiple Coulomb scattering. For a track with no dip the fractional uncertainty in momentum is approximately $0.295/\beta\sqrt{l}$ in this chamber, where l is the length of the track in centimeters.[30] For a typical track 10 cm in length the uncertainty is 10% or more. A track of minimum

[29] W. D. Shephard, Ph.D., thesis, University of Wisconsin, 1962 (unpublished).

[30] D. V. Bugg, *Progress in Nuclear Physics* (Pergamon Press, New York, 1959), Vol. 7, p. 42.

acceptable length, 5 cm, would have an uncertainty in momentum of 13% or more. The next largest source of error is the experimental determination of radii of curvature. This is estimated for each measurement and is generally on the order of 5%. Other errors are small in comparison to these.

Several checks were made on the accuracy of momentum measurements. Momentum determinations by range and by curvature were compared for a group of stopping tracks more than 10 cm long. Rough corrections were made for energy loss along the track. Out of 28 cases checked, there were 20 cases where agreement was better than 10%. In most of the others the two methods agreed to within 20%. The agreement of the elastic scattering results of this experiment with the results of Leitner,[28] where momentum measurements were not used, would tend to imply that no large systematic errors in momentum determination exist.

In the kinematic analysis a figure of 10% was used for the momentum uncertainty on all tracks where measurement uncertainties did not exceed this value. This restriction may result in a loss of good hydrogen events but should produce no systematic errors.

Carbon contamination of elastic scattering in the experiment of Leitner[28], where momenta were not measured, was estimated as $(4\pm2)\%$. The same figure is used for elastic scatterings in this experiment.

Carbon contamination must be estimated separately for the single pion production events, which are not as overdetermined by the measurements as are elastic scattering events. An estimate of the carbon contamination has been formed from an analysis of 52 $(---+)$ stars which must be predominantly $\pi^-+n\rightarrow\pi^-+\pi^-+p$ events involving a neutron in the carbon nucleus. Kinematically these events should resemble single pion productions involving protons in carbon. Measurement procedures were identical to those for $(-+)$ events. These events were first analyzed to see if momentum and energy would balance within errors as they should if the events had involved nucleons at rest. In only 3 cases out of the 52 could a balance be obtained. The events were then analyzed by considering two secondaries at a time and analyzing the events in the same way as the $(-+)$ events (i.e., assuming the "+" to be either a pion or a proton). Thus, there were available 208 of these pairs for analysis—104 which consist of two pions and 104 which consist of a pion and a nucleon. In 28 of these 208 cases, the criteria for single pion production in hydrogen applied to the $(-+)$ events were satisfied. In 20 of these cases, the nature of the "positive" secondary was correctly identified. Of the 8 remaining cases, 3 were kinematically ambiguous, and 5 resulted in incorrect identifications. From these numbers the carbon contamination in the single pion production events can be estimated. It is estimated that $(13.4\pm3)\%$ of the single pion productions in carbon might have appeared to be events in hydrogen under the analysis used in this experiment.

Of the 1092 measurable $(-+)$ events in the fiducial region, 460 were classified as hydrogen events and 632 as carbon events. Assuming the same proportions of elastic and single pion production events in carbon as determined in hydrogen and making an allowance for the fact that some elastic events in carbon might appear to be single pion productions in hydrogen, it is estimated that $(15\pm5)\%$ of the events classified as hydrogen events may be carbon events. The error is taken as larger than statistical to allow for uncertainties in the assumptions. From the results of the $(---+)$ study, the portion of carbon contamination representing cases where the reaction scheme is incorrectly identified should be less than about 3% of the total number of single pion productions. Thus, the effect of carbon contamination on the branching ratio determined for π^+ and π^0 production should be considerably less than the effect on the determination of cross sections for the processes. The effect of the small contamination of bound proton events on the distributions is probably small indeed. The result of including such cases is that the effective beam momentum is spread over a wider range than the true beam momentum.

No clear method of estimating the number of good hydrogen interactions rejected due to the stringent acceptance criteria for hydrogen events has been found. It is estimated that an upper limit on the number of additional events which might have been accepted as hydrogen events with momentum variations of 15–20% would be about 30% of the events accepted with present limits.

As Baggett[17] has pointed out, there is an ambiguity between π^+ and π^0 production, even for the case of definite hydrogen events in events where the laboratory momenta of the positive and neutral secondaries are equal. The region of kinematic ambiguity about $p_+=p_0$ widens as uncertainties in measurements increase. In 31 out of 437 single pion production cases p_+ and p_0 differed by less than 10%. The positive particle could be identified by bubble density in 20 of these cases. In 8 other cases some other feature permitted identification. A number of other cases were kinematically ambiguous due to uncertainties in angles but only 2 could not be identified by other means. Thus a total of only 5 events were classified as either π^+ or π^0 production.

Selection criteria can be checked by examining the spectra of initial neutral particle masses for cases classified as single pion production to see if peaks occur at π^0 and neutron masses. In order to avoid the problem of distortion in the spectra for low mass values due to the fact that a small change in E_0 or P_0 can cause a large change in the neutral mass for $M_0=(E_0^2-P_0^2)^{\frac{1}{2}}\approx0$, plots for M_0^2 rather than M_0 were used. These plots are shown in Fig. 1. The spectra show peaks at the right mass values. The rms neutral mass for $\pi^-+p\rightarrow\pi^-+\pi^++n$ events is 940.4 Mev/c^2 and for $\pi^-+p\rightarrow\pi^-+\pi^0+p$ events is 133.2 Mev/c^2. In both

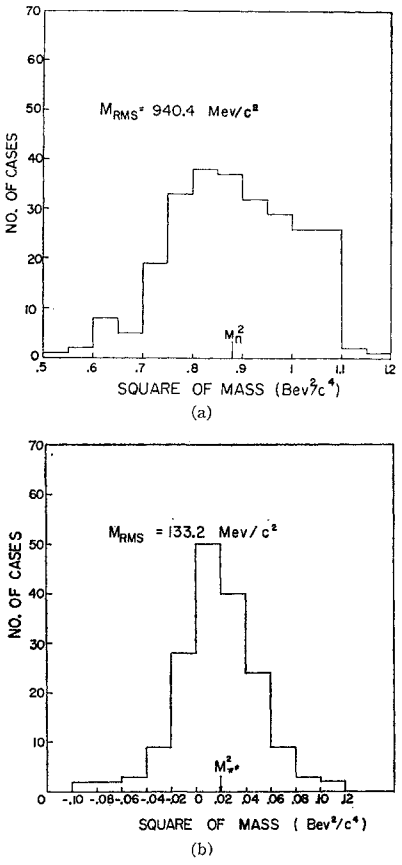

FIG. 1. Distribution of squares of initially determined masses of neutral particles, (a) from events classified as $\pi^-+p\rightarrow\pi^-+\pi^++n$; (b) from events classified as $\pi^-+p\rightarrow\pi^-+\pi^0+p$.

cases the width of the peak at half maximum corresponds to about ± 100 Mev/c^2. The agreement of the rms masses with accepted masses for the neutron and neutral pion is excellent.

IV. CORRECTIONS

Before going further it is necessary to make corrections, both specific and general, to the data. An apparent pion path length for the experiment can be calculated from counts of the number of beam tracks passing through the fiducial region. In principle one can then calculate the cross section for various types of reactions from a knowledge of the number of reactions and density of the hydrogen in the chamber. There are however numerous corrections to be made which are listed below.

Corrections have been made for the following effects:

1. μ and e contamination of the beam. $C_\mu=0.935\pm0.04$ taken from Cool *et al.*[31]

2. Scanning efficiency. In this case about 20% of the film was double scanned, and the efficiency estimated from the overlap of events in the fiducial region. The results are given in Table I for each type of event.

TABLE I. Scanning corrections for fiducial region.

Event type	Scanning correction
$(-+)$ star	1.14 ± 0.10
$(--++)$ star	$1.25_{-0.25}^{+0.67}$
Track ending	1.59 ± 0.30
$(--+)$ star	$1.40_{-0.40}^{+0.60}$
Carbon star	$1.03_{-0.03}^{+0.10}$
Track deflection	1.72 ± 0.23

3. Correction for inhomogeneity of the position of events in the $X-Y$ plane of the fiducial region of the chamber. Figure 2 shows the distribution of $(-+)$ events. There are too few events on the far right apparently, because the outgoing tracks fail to meet the measurement criteria. A correction factor of $C_{X-Y}=1.17\pm0.20$ is used to correct a similar effect for track endings, since no stoppings could fail to satisfy measurement criteria.

4. Carbon contamination corrections are $C_B=0.96\pm0.02$ for elastic events $C_B=0.85\pm0.05$ for single pion production. These number have been estimated above.

5. Corrections were made for the fact that some events in the fiducial region are unmeasurable: $C_U(-+)=1.21\pm0.08$, and $C_U(--++)=1.46\pm0.25$.

6. Special corrections can be made to elastic scatterings. These come about because of scanning inefficiencies which are dependent on the azimuth of the plane containing the π and scattered proton. Since the distribution in azimuth should be uniform, a correction can be computed from the lack of uniformity. This is done for events with $0.90>\cos\theta_\pi^*\geqslant-1.0$ and $0.95>\cos\theta_\pi^*\geqslant0.90$ and the $C_\phi=1.37\pm0.08$ and 1.57 ± 0.15, respectively. For cases with $1.0\geqslant\cos\theta_\pi^*\geqslant0.95$ the correction is made on the basis of dispersion theory by

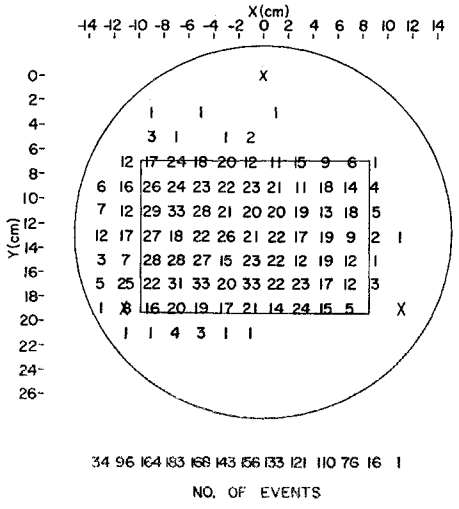

FIG. 2. $X-Y$ distribution of event positions for 1401 measurable two-prong events.

[31] R. Cool, O. Piccioni, and D. Clark, Phys. Rev. **103**, 1082 (1956).

computing $d\sigma/d\Omega(0°) = 10.6 \pm 0.6$ mb/sr. By extrapolating from the last measured point it is found that 90 ± 17 events should have been in the last interval.

V. CROSS SECTIONS

To measure the total pion path length scanned, tracks traversing the fiducial region were counted in every fifth picture. Pictures with no tracks or with too many tracks for accurate scanning were eliminated. When corrected for muon and electron contamination, the pion path length is 6.473×10^5 cm $\pm 4.3\%$. Cross sections are calculated from the scanning data by using this number and the calculated correction factors from Sec. IV.

Table II contains the numbers of events found in scanning and measured both inside the fiducial region and in the whole chamber.

In Table III are listed the absolute experimental cross sections from this experiment and from other experiments for processes involving 1.3-Bev $\pi^- - p$ and $\pi^- - C$ interactions. The cross sections measured in other experiments are in general somewhat larger than the cross sections from this experiment. It seems probable that this is due to the loss of good hydrogen interactions because of the stringent selection criteria. No correction for such an effect has been made.

Estimates of cross sections can be made by using the ratios found in this experiment and the values of total, elastic, and neutral particle[32] cross sections from other experiments. The elastic cross-section value of Leitner[5,28] has been corrected using the newer values of the total cross section to calculate the correction for small-angle scattering. It then becomes 10.5 ± 0.8 mb. The results for the corrected cross sections from this experiment are combined with the results of the other experiments in Table IV to give what are believed to be the best values for $\pi^- - p$ interaction cross sections at 1.3 Bev currently available. The same correction factor is used for all types of $(-+)$ events and is derived from the ratio of the measured elastic scattering cross sections. The elastic scattering angular distribution from this experiment is consistent with that of Leitner. A somewhat larger correction is used for the $(--++)$ events, since a larger fraction of hydrogen events has probably been rejected.

The value listed for multiple pion productions involving two neutrals is that required to give the desired total cross section. An average of the measurements from Berkeley[1] and from Saclay[2] is used for the total cross section.

The only quantity calculated for $\pi^- - C$ interactions in this experiment is the total cross section—301_{-22}^{+24} mb. This value must include some hydrogen interactions, and no correction has been made for small-angle deflections which must have been missed. The value can be compared qualitatively with measurements by Cronin *et al.*[33] of $\pi^- - C$ cross sections up to 1.2 Bev. They measured an absorption cross section of 246 ± 14 mb and a diffraction cross section of 105 ± 22 mb at 1.2 Bev.

TABLE II. Classification of events in this experiment.

Event classification	Events in fiducial region	Total events measured
I. $(-+)$ events	1321	1401
A. (π^-,p) elastic	116	150
B. (π^-,π^0,p)	133	173
C. (π^-,π^+,n)	206	259
D. (π^-,π^0,p) or (π^-,π^+,n)	5	5
E. All $(-+)$ hydrogen events	460	587
F. $(-+)$ carbon events	632	814
G. Not measurable	229	···
II. $(--++)$ events	59	77
A. (π^-,π^-,π^+,p)	12	16
B. Carbon interactions	47	61
III. Track endings	185	···
IV. $(--+)$ events	53	···
V. Other stars	1229	···
VI. Deflections	506	···

TABLE III. Experimental cross sections.

Interaction	Absolute cross section from this experiment (mb)	Absolute cross section from other experiments (mb)
$\pi^- + p \to \pi^- + p$	9.1 ± 1.2	10.1 ± 0.8[b]
$\pi^- + p \to \pi^- + \pi^0 + p$	5.4 ± 0.8	
$\pi^- + p \to \pi^- + \pi^+ + n$	8.0 ± 1.2	
$\pi^- + p \to \pi^- + \pi^- + \pi^+ + p$	$0.7_{-0.2}^{+0.4}$	
$\pi^- + p \to \begin{cases} \pi^- + \pi^0 + \pi^0 + p \\ \pi^- + \pi^+ + \pi^0 + n \end{cases}$	$1.4_{-0.6}^{+1.2}$[a]	
$\pi^- + p \to \begin{cases} \pi^0 + n \\ \pi^0 + \pi^0 + n \\ \pi^0 + \pi^0 + \pi^0 + n \\ Y^0 + K^0 \end{cases}$	4.7 ± 1.4	5.2 ± 0.2[c]
$\pi^- + p \to Y^0 + K^0$	···	0.56 ± 0.80[d]
$\pi^- + p \to \Sigma^- + K^+$	···	0.23 ± 0.04[d]
$\pi^- + p \to$ observed processes	27.9 ± 2.9	
Total cross section	$29.3_{-3.0}^{+3.1}$	34.5 ± 1.1[e] 34.9 ± 1.4[f]
$\pi^- - C$	301_{-22}^{+24}	

[a] Estimated from measured value of $\sigma(\pi^- + p \to \pi^- + \pi^- + \pi^+ + p)$ and theoretical predictions.
[b] See references 5 and 28.
[c] See reference 32.
[d] See reference 26.
[e] See reference 1.
[f] See reference 2.

VI. SINGLE PION PRODUCTION

The major effort in this experiment has gone into the study of single pion production interactions and the comparison of the experimental results with theory.

[32] J. C. Brisson, P. Falk-Variant, J. P. Merlo, P. Sonderegger, P. Turlay, and G. Valladas, *Proceedings of the 1960 Annual International Conference on High-Energy Physics at Rochester* (Interscience Publishers, Inc., New York, 1960), p. 191.

[33] J. Cronin, R. Cool, and A. Abashian, Phys. Rev. **107**, 1121 (1957).

TABLE IV. 1.3-Bev $\pi^- - p$ interaction cross sections.

Interaction	Cross section (mb)
$\pi^- - p$ total cross section	34.7 ±1.2
$\pi^- + p \rightarrow \pi^- + p$	10.5 ±0.8
$\pi^- + p \rightarrow \pi^- + \pi^0 + p$	6.2 ±0.9
$\pi^- + p \rightarrow \pi^- + \pi^+ + n$	9.2 ±1.4
$\pi^- + p \rightarrow$ neutral particles	5.2 ±0.2
$\pi^- + p \rightarrow Y^0 + K^0$	0.56±0.08
$\pi^- + p \rightarrow \begin{cases} \pi^0 + n \\ \pi^0 + \pi^0 + n \\ \pi^0 + \pi^0 + \pi^0 + n \end{cases}$	4.6 ±0.2
$\pi^- + p \rightarrow \Sigma^- + K^+$	0.23±0.04
$\pi^- + p \rightarrow \pi^- + \pi^- + \pi^+ + p$	$1.0_{-0.3}^{+0.5}$
$\pi^- + p \rightarrow \begin{cases} \pi^- + \pi^0 + \pi^0 + p \\ \pi^- + \pi^+ + \pi^0 + n \end{cases}$	2.4 ±2.2

The general experimental results will be presented followed by detailed comparisons with three models or theories—the statistical model, the isobar model of Lindenbaum and Sternheimer, and the pion-pion interaction theory involving single pion exchange.

A. Experimental Results

The possible single pion production interactions in $\pi^- - p$ collisions are:

$$\pi^- + p \rightarrow \pi^- + \pi^+ + n, \quad \text{(I)}$$

$$\pi^- + p \rightarrow \pi^- + \pi^0 + p, \quad \text{(II)}$$

$$\pi^- + p \rightarrow \pi^0 + \pi^0 + n. \quad \text{(III)}$$

Only the first two could be studied in detail in the experiment. The branching ratio for the first two processes is $R = \sigma^{II}/\sigma^{I} = 0.668 \pm 0.066$. An upper limit on the cross section for reaction (III) is given by the cross section for all reactions involving only neutral pions and neutrons as 4.6±0.2 mb. Since a considerable fraction of these events must be charge-exchange scatterings, the cross section for (III) is probably on the order of 2 mb.

The most compact way of presenting the data is in the form of scatter diagrams of center-of-mass (c.m.) momenta and angles for each type of secondary particle. These are presented in Figs. 3 and 4. They are useful for the detection of angle-momentum correlations. But for detailed comparison with theoretical curves it is necessary to use projections of the scatter diagrams and other presentations of the data. These are presented in the comparisons with theories as required.

B. Statistical Model

The statistical model as developed by Fermi[34] forms a starting point for comparison with theory. Probabilities for various possible final states are determined by the conservation laws and by the statistical weights of the states. The c.m. angular distributions are expected to be symmetric about 90° and the momentum distributions are given by the three-body phase-space factors.

The experimental angular distributions are clearly not symmetric about 90°, and the momentum distributions are not in good agreement with the phase-space predictions in most cases. Angular distributions for the secondaries are presented in Figs. 10 to 12 for different ranges of four-momentum transfer to the nucleon.

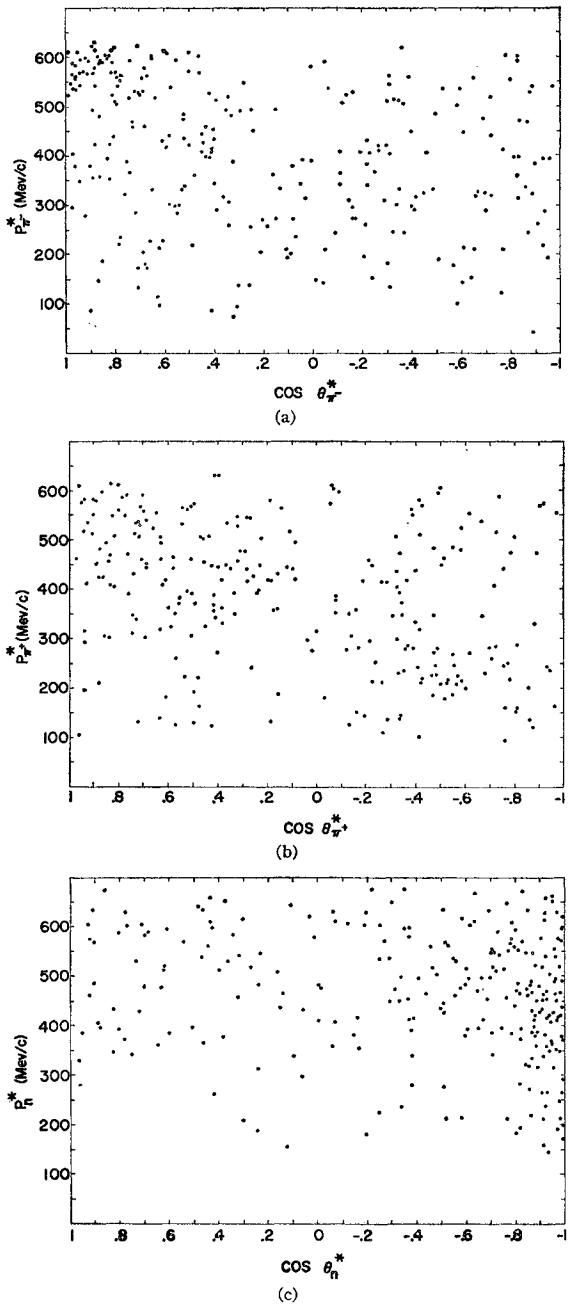

FIG. 3. Scatter diagrams of c.m. momenta and angles for secondary particles in 259 events classified as $\pi^- + p \rightarrow \pi^- + \pi^+ + n$. The diagrams are shown, (a) for π^-, (b) for π^+, and (c) for n.

[34] E. Fermi, Progr. Theoret. Phys. (Kyoto) 5, 570 (1950).

Although the statistical model is not satisfactory for many features of the interactions, it is instructive to compare the momentum distributions from three-body phase space with the experimental data as a reference point for evaluation of the validity of the isobar model predictions. The phase-space distributions have been calculated from the expressions published by Block.[35] The distributions are shown as solid curves in Figs. 7 and 8.

C. Isobar Model

The Lindenbaum-Sternheimer isobaric nucleon model or isobar model[8–12] has been used for several years in an attempt to use the $T=J=\frac{3}{2}$ pion-nucleon resonance to explain some features of pion production in the Bev region. The single-level model[10] has been applied by Derado and Schmitz[19] and Alles-Borelli *et al.*[18] to data from experiments near 1 Bev with some success.

Predictions of the isobar model have been compared to the results of this experiment. In order to eliminate some of the variable parameters, use was made of preliminary results by the Yale bubble chamber group on 1.26-Bev $\pi^+ - p$ interactions.[36] Cross sections for the $\pi^+ - p$ interactions involved are listed in Table V. The cross sections have been normalized to a counter value of 39.7 mb for the total cross section.

With the use of these data, there are no remaining undetermined parameters in the model to allow the fitting of the theoretical momentum spectra to the experimental values. The isobar model momentum spectra are obtained from a combination of spectra $J_{\pi,1}$ for decay pions from the isobar and $J_{\pi,2}$ for recoil pions from the reaction producing the isobar. The spectra involved are shown in Fig. 5. The details of the model have been published by Lindenbaum and Sternheimer,[10] so only enough will be given here to indicate the nature of the calculations.

The relative proportions of the two pion spectra are specified by two parameters, ρ and a, where

$$\rho=\sigma_{\frac{3}{2},\text{inel}}/2\sigma_{\frac{1}{2},\text{inel}}$$

relates the $T=\frac{3}{2}$ and $T=\frac{1}{2}$ inelastic cross sections and

$$a=2(\rho/5)^{\frac{1}{2}}\cos\phi,$$

TABLE V. $\pi^+ - p$ interaction cross sections at 1.26 Bev.

Interaction	Cross section (mb)
$\pi^+ + p \rightarrow \pi^+ + p$	16.4±1.4
$\pi^+ + p \rightarrow \pi^+ + \pi^0 + p$	11.8±1.2
$\pi^+ + p \rightarrow \pi^+ + \pi^+ + n$	4.6±0.7
$\pi^+ + p \rightarrow$ multiple pion production	6.9±0.9
$\pi^+ + p$ total cross section	39.7

[35] M. M. Block, Phys. Rev. **101**, 796 (1956).

[36] Private communications from H. Courant. The cross sections from preliminary results, which were used in the calculations of this article, differ slightly but not significantly from cross sections published in reference 39.

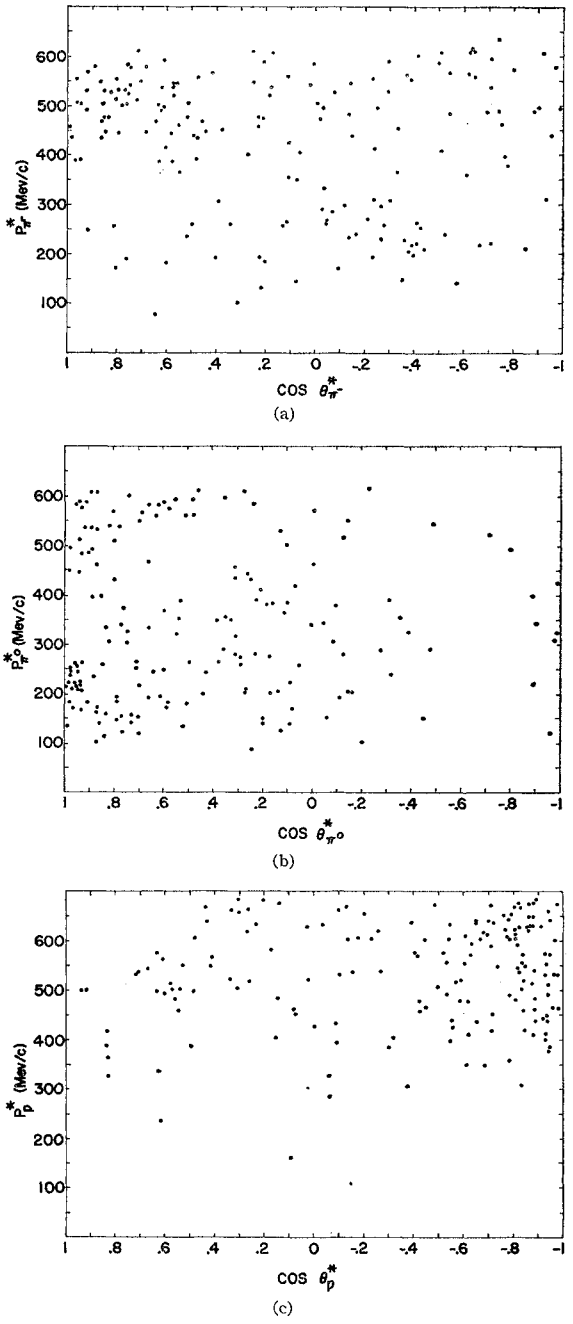

FIG. 4. Scatter diagrams of c.m. momenta and angles for secondary particles in 173 events classified as $\pi^- + p \rightarrow \pi^- + \pi^0 + p$. The diagrams are shown, (a) for π^-, (b) for π^0, and (c) for p.

where ϕ is the phase difference between matrix elements for producing the isobar in the $T=\frac{1}{2}$ and $T=\frac{3}{2}$ states. From the Yale data we have $\sigma_{\frac{3}{2},\text{inel}}=23.3$ mb, and from a combination of Yale data and the data of this experiment we obtain $\sigma_{\frac{1}{2},\text{inel}}=19.0$ mb. The latter figure was arrived at by assuming that approximately 40% of the events with neutral secondaries were inelastic events. This assumption seems to be reasonable, and any errors

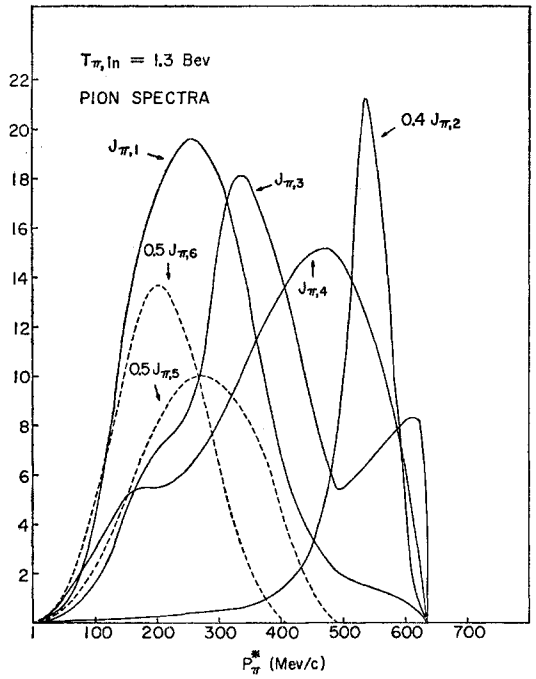

FIG. 5. Pion spectra for $T_{\pi,\mathrm{in}}=1.3$ Bev for the isobar model.

involved are not expected to influence the results significantly. Then we have $\rho=0.613$. The value for ϕ is obtained from the ratio of π^0 to π^+ production:

$$R=\sigma(\pi^-,\pi^0,p)/\sigma(\pi^-,\pi^+,n)$$
$$=(10+17\rho-25a)/(25+26\rho+35a).$$

By inserting the value $\rho=0.613$ and the experimental ratio $R=0.668$ into this expression one finds $a=-0.149$, corresponding to $\phi=102.3°$. The momentum spectra have been calculated from these parameters and compared with the experimental distributions. Agreement was not good, especially for the π^+ distribution where a much larger peak at 540 Mev/c is predicted than is observed.

The spectra for the one-level model are not published, since somewhat better agreement with experiment can be obtained using an extension of the model including effects of $T=\frac{1}{2}$ isobaric states corresponding to observed resonances at 600 and 880 Mev in the π^-p cross section. The extended model allows the description of double pion production in addition to single production. Additional parameters are available for variation but, by using most of the cross sections measured for both π^-p and π^+p interactions, it is possible to avoid direct reference to the experimental momentum spectra in calculating the theoretical spectra.

The relations involving the cross sections, the theoretical momentum spectra, and the parameters used to describe them are quite lengthy and are described in detail in the paper by Sternheimer and Lindenbaum.[12] The methods of calculation used in this experiment will be described very briefly. The theoretical curves used to compute the spectra are shown in Figs. 5 and 6. They were calculated by Sternheimer. From the cross sections for single and multiple pion production in the Yale experiment and in this experiment, values were calculated for cross sections for production of the different isobars in the two possible isotopic spin states and the fraction of the $T=\frac{1}{2}$ isobar decaying via single and double pion production modes. Parameters involving these quantities which were needed in the calculation of the theoretical spectra were then calculated in a manner similar in principle to that used for the single-level model. The basic parameters are ρ_1 and ϕ_1, ρ_2 and ϕ_2, where these terms have the same significance for the $T=\frac{3}{2}$ and $T=\frac{1}{2}$ isobaric states, respectively, as ρ and ϕ did in the single-level model. Results for the different cross sections and parameters are listed in Table VI. The notation used for the cross sections is $\sigma_{2T,\alpha}$ where T is the isotopic spin and $\alpha=1$ refers to the $T=\frac{3}{2}$ isobar, $\alpha=2$ to the $T=\frac{1}{2}$ isobar (see reference 12). An additional subscript s or d refers to single or double pion production. The parameters were found by solving as simultaneous equations the four relations given by Sternheimer and Lindenbaum for σ_{12} in terms of $\sigma_{12,s}$ and $\sigma_{12,d}$ and for the cross sections $\sigma(\pi^-,\pi^+,n)$, $\sigma(\pi^-,\pi^0,p)$, and $\sigma(\pi^-,\pi^-,\pi^+,p)$ in terms of the $\sigma_{2T,\alpha}$ and the parameters. It was assumed that $\rho_1=\rho_2$ as Sternheimer has assumed in his published calculations. A useful additional parameter is $k=\sigma_{32}/(\sigma_{31}+\sigma_{32})=\sigma_{12}/(\sigma_{11}+\sigma_{12})$, which gives the fraction of events involving the $T=\frac{1}{2}$ isobar. In this experiment a value of $k=0.491$ was calculated which would indicate

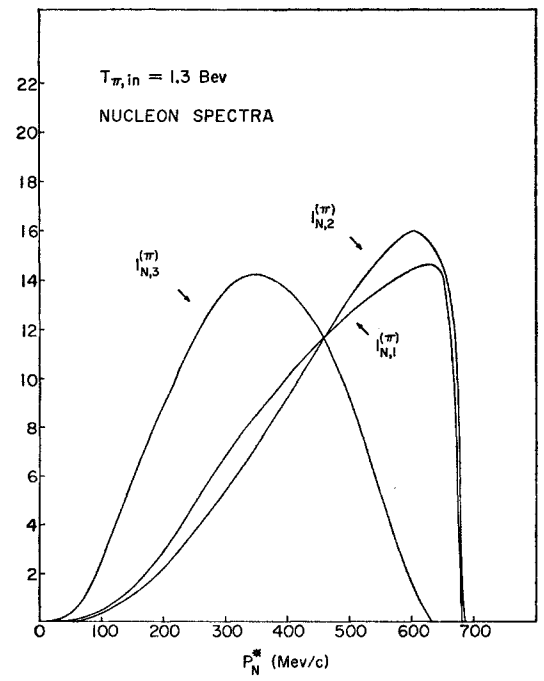

FIG. 6. Nucleon spectra for $T_{\pi,\mathrm{in}}=1.3$ Bev for the isobar model.

TABLE VI. Isobar model cross sections and parameters.

Parameter or cross section	Value used or determined
I. Cross sections (in mb) from experiment	
$\sigma(\pi^-,\pi^+,n)$	9.2
$\sigma(\pi^-,\pi^0,p)$	6.2
$\sigma(\pi^-,\pi^-,\pi^+,p)$	1.0
$\sigma(\pi^+,\pi^0,p)$	11.8
$\sigma(\pi^+,\pi^+,n)$	4.6
$\sigma(\pi^+-p$ multiple production)	6.9
$\sigma_{\frac{3}{2},\text{inel}}$	23.3
$\sigma_{\frac{1}{2},\text{inel}}$	19.0
II. Cross sections (in mb) calculated	
σ_{31}	11.84
σ_{32}	11.46
$\sigma_{32,s}$	4.56
$\sigma_{32,d}$	6.9
σ_{11}	9.65
σ_{12}	9.35
$\sigma_{12,s}$	6.94
$\sigma_{12,d}$	2.41
III. Parameters calculated	
$\rho_1=\rho_2$	0.613
$\cos\phi_1$	−0.021
$\cos\phi_2$	0.339
k	0.491
a	−0.023
A	1.122
B	0.492

that about half of the events involved the $T=\frac{1}{2}$ isobar. Further details of the calculations are given in reference 29.

Figures 7 and 8 show the experimental momentum distributions for secondary particles along with the

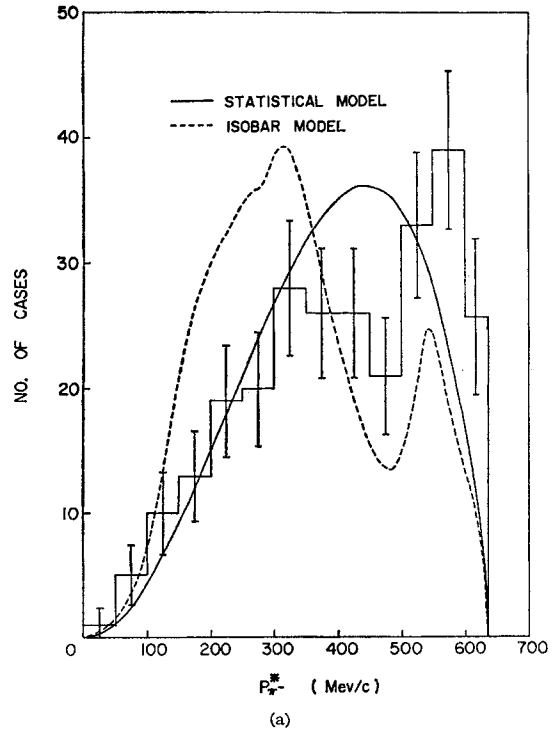

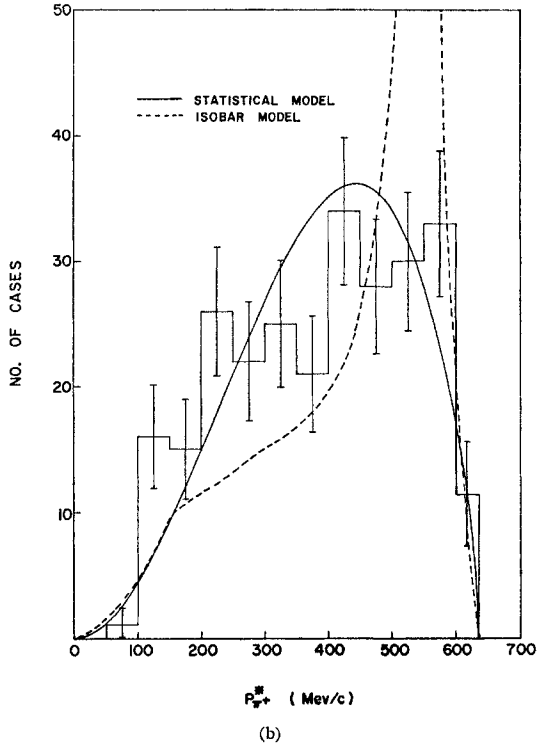

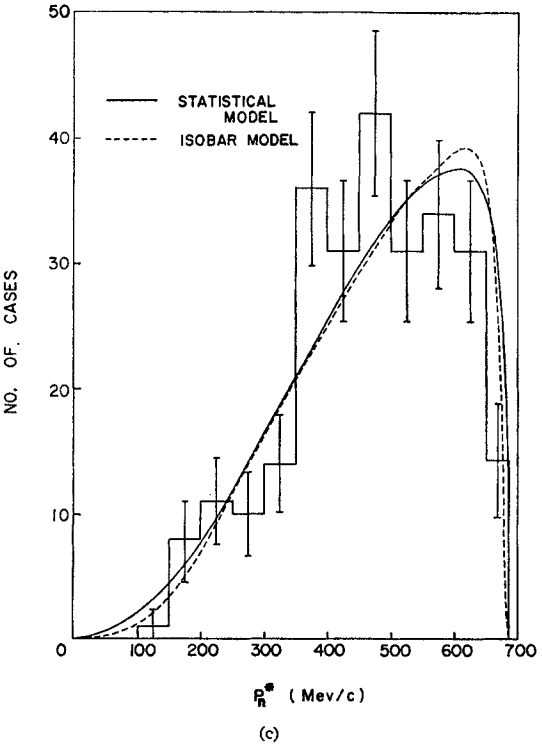

FIG. 7. Center-of-mass momentum distributions for secondary particles in 259 $\pi^-+p\rightarrow\pi^-+\pi^++n$ events. Distributions are shown, (a) for π^-, (b) for π^+, and (c) for n. The solid curves are calculated for the statistical model; the dashed curves are for the extended isobar model.

phase-space distributions and the distributions calculated from the extended isobar model using the parameters in Table VI. These theoretical distributions were calculated using the best available values for the partial cross sections required. The isobar-model distributions are in somewhat better agreement with the data than are the phase-space curves. The largest source of disagreement is still the π^+ peak at 540 Mev. As a qualitative test of the goodness of fit between experimental and calculated theoretical distributions χ^2 values were calculated for each distribution and for all distributions combined. These indicate that, although the isobar model gives a somewhat better fit than the statistical model, neither provides a good quantitative fit to the data. For all distributions combined (80 deg of freedom) the values are $\chi^2=274$ for the isobar model and 309 for the statistical model. The statistical model provides a somewhat better fit to the (π^-,π^+,n) events than does the isobar model ($\chi^2=82.9$ vs $\chi^2=165$ for 40 deg of freedom). The poorness of fit of the theory indicates a lack of any real quantitative agreement.

Uncertainties in the isobar-model parameters resulting from uncertainties in the input data were not calculated in detail. Some of them appear to be quite large. Because of the large number of parameters involved, no systematic attempt was made to find a best fit to the combined cross section and momentum data. Some variations were performed, and better fits to the momentum distributions without definite disagreement with cross sections were found. By using listed values of $\sigma(\pi^-,\pi^+,n)$, $\sigma(\pi^-,\pi^0,p)$, $\sigma_{\frac{1}{2},\text{inel}}$, $\sigma_{\frac{3}{2},\text{inel}}$,

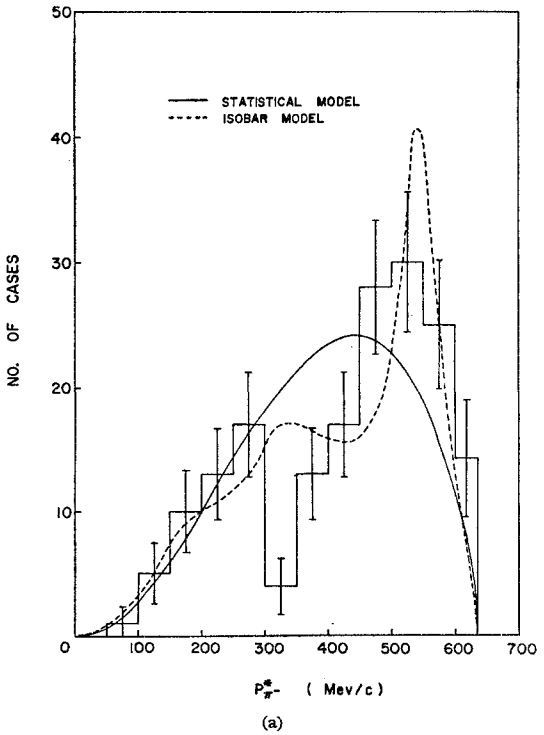

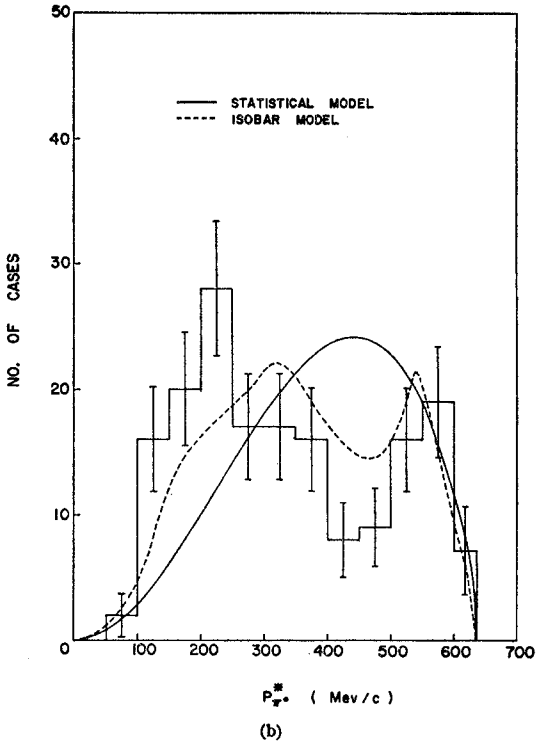

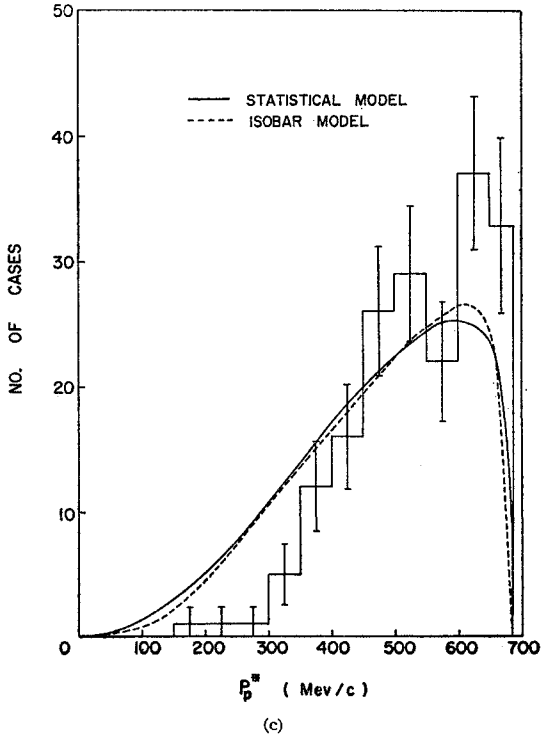

FIG. 8. Center-of-mass momentum distributions for secondary particles in 173 $\pi^-+p\rightarrow\pi^-+\pi^0+p$ events. Distributions are shown, (a) for π^-, (b) for π^0, and (c) for p. The solid curves are calculated for the statistical model; the dashed curves are for the extended isobar model.

and by varying k and $\cos\phi_2$ it was found that the large π^+ peak could be reduced. With $k=0.6$ and $\cos\phi_2=1.0$ the fit to the π^+ distribution was considerably improved but the over-all fit was still poor ($\chi^2=215$ for 80 deg of freedom). Further improvement might be possible, but a really good quantitative fit seems improbable.

Two-particle Q-value distributions have been examined to see if peaks in pion-nucleon Q values occur corresponding to the expected masses of the assumed isobaric states. These are $Q(\pi,p)=150$ Mev for the $T=\frac{3}{2}$ isobar and 430 and 600 Mev for the $T=\frac{1}{2}$ levels. Since for a three-body final state the Q value for two particles is determined by the momentum of the third, the over-all agreement between experimental and theoretical Q-value distribution cannot be significantly better than that for the momentum distributions. The observed 150-Mev $Q(\pi^-,n)$ peak is smaller and the $Q(\pi^+,n)$ peak larger than those predicted by the isobar model. No significant higher peaks are observed. Predicted higher peaks are missing in the $Q(\pi^0,p)$ distribution.

No detailed predictions of angular distributions for secondaries have been made from the isobar model. Such predictions would depend on further assumptions about the angular momentum states involved.

D. Pion-Pion Interactions

The dominant feature of $\pi-p$ interactions above a few hundred Mev is the predominance of interactions involving small momentum transfers to the nucleon. They can be explained most easily in terms of an interaction of the incoming pion with a pion in the cloud of the nucleon. Selleri has briefly summarized some of the history of speculation about pion-pion interactions in an article discussing evidence for $\pi-\pi$ resonances.[37] A number of authors have considered the effects of $\pi-\pi$ interactions on $\pi-p$ interactions and have suggested ways of experimentally detecting $\pi-\pi$ resonances and obtaining data on the $\pi-\pi$ cross section and the nature of any resonance.[13–16,38] Several papers have been published recently in which the theoretical suggestions are applied to $\pi^- - p$ data near 1 Bev.[18,20,22,23,39] Some effects were observed which might be interpreted as indicating a resonance with a total energy for the $\pi-\pi$ system in the region from 500 to 700 Mev.

Erwin *et al.*[16] have observed a $\pi-\pi$ resonance in the $T=1$ state at about 765 Mev in a study of 1.89-Bev/c $\pi^- - p$ interactions. This is also observed in the $\pi^+ - p$ study by the Yale group[39] whose results also seem to rule out the presence of a $T=2$ resonance in this region, and in a $\pi^- - p$ study at 1.03 Bev/c at the Bevatron.[40]

[37] F. Selleri, Nuovo cimento **16**, 775 (1960).
[38] F. Salzman and G. Salzman, Phys. Rev. **120**, 599 (1960).
[39] D. Stonehill, C. Baltay, H. Courant, W. Fickinger, E. C. Fowler, H. Kraybill, J. Sandweiss, J. Sanford, and H. Taft, Phys. Rev. Letters **6**, 624 (1961).
[40] J. A. Anderson, V. X. Bang, P. G. Burke, D. D. Carmony, and M. Schmitz, Phys. Rev. Letters **6**, 365 (1961).

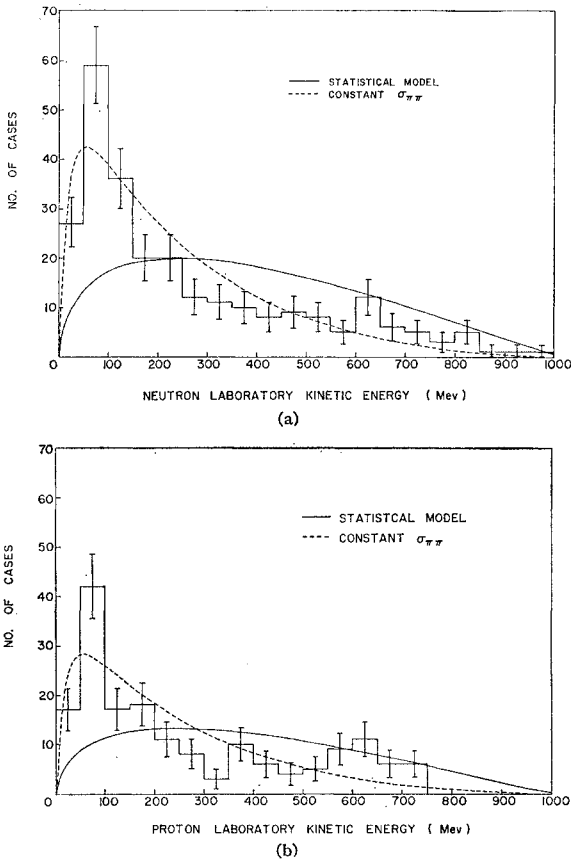

FIG. 9. Laboratory system kinetic energy distributions for nucleons in single pion production events. Distributions are shown, (a) for n from $\pi^- + p \to \pi^- + \pi^+ + n$, and (b) for p from $\pi^- + p \to \pi^- + \pi^0 + p$. The solid curves are calculated for the statistical model; the dashed curves are for a $\pi-\pi$ interaction with constant $\sigma_{\pi\pi}$.

Selleri[37] has commented that the idea that the $\pi-\pi$ interaction is the dominant effect in single pion production does not necessarily conflict with the fact that the isobar model tends to explain some of the experimental observations near 1 Bev. Effects of the $T=J=\frac{3}{2}$ resonance should be quite evident since, with the total energy distributed among three particles, the energy of either secondary pion relative to the nucleon has a high probability of being near the resonance. Also the dimensions of the pion wave packets are such that they should partially overlap the nucleon core. Thus a final-state $\pi-N$ interaction is quite likely to occur in the $T=J=\frac{3}{2}$ state. This would not, however, be expected to happen in every case, and it might be hoped that the cases where rescattering does not occur could be selected in some manner.

The data of this experiment have been examined for evidence of a $\pi-\pi$ interaction and evidence has been found. Goebel[13] has suggested that the presence of a strong $\pi-\pi$ interaction would result in a low-energy peak in the laboratory kinetic energy spectrum of the nucleons in pion production events. Figure 9 shows the

TABLE VII. Relative probabilities of final states.

Interaction	$T=0$	$T=1$	$T=2$	1.3-Bev π^-+p cross sections all Δ	1.3-Bev π^-+p cross sections $\Delta\leqslant 550$ Mev/c	1.26-Bev π^++p cross sections
$\pi^-+p\rightarrow\pi^-+\pi^++n$	2/9	1/2	1/18	9.2±1.4 mb	4.5±0.7 mb	
$\pi^-+p\rightarrow\pi^-+\pi^0+p$	0	1/4	1/4	6.2±0.9 mb	2.9±0.7 mb	
$\pi^-+p\rightarrow\pi^0+\pi^0+n$	1/9	0	1/9	~2.5 mb		
$\pi^++p\rightarrow\pi^++\pi^++n$	0	0	2			4.6 mb
$\pi^++p\rightarrow\pi^++\pi^0+p$	0	1/4	1/4			11.8 mb

laboratory kinetic energy spectra for nucleons in (π^-,π^+,n) and (π^-,π^0,p) final state, respectively. Both distributions exhibit definite peaks in the region from 50 to 100 Mev. The solid curve is calculated from three-body phase space factors, and the dashed curve is the spectrum predicted by the formula presented by Chew and Low[14] for single pion production via a pion-pion interaction. The formula is

$$\frac{\partial^2\sigma}{\partial\Delta^2\partial\omega^2}=\frac{\alpha f^2}{2\pi}\frac{\Delta^2/\mu^2}{(\Delta^2+\mu^2)^2}\frac{1}{q_{1L}{}^2}\omega(\tfrac{1}{4}\omega^2-\mu^2)^{\frac{1}{2}}\sigma_{\pi\pi}(\omega),$$

where Δ^2 is the four-momentum transfer to the nucleus, ω is the total energy in the $\pi-\pi$ c.m. system, q_{1L} is the laboratory momentum of the incident pion, μ is the pion mass, and α is 1 for (π^-,π^0,p) and 2 for (π^-,π^+,n). The formula is expected to be valid in the unphysical limit where Δ^2 approaches $-\mu^2$. In calculating the dashed curve, $\sigma_{\pi\pi}(\omega)$, the $\pi-\pi$ interaction cross section, was assumed to be constant. This is not a reasonable assumption, but the resulting distributions illustrate the expected low-energy peak.

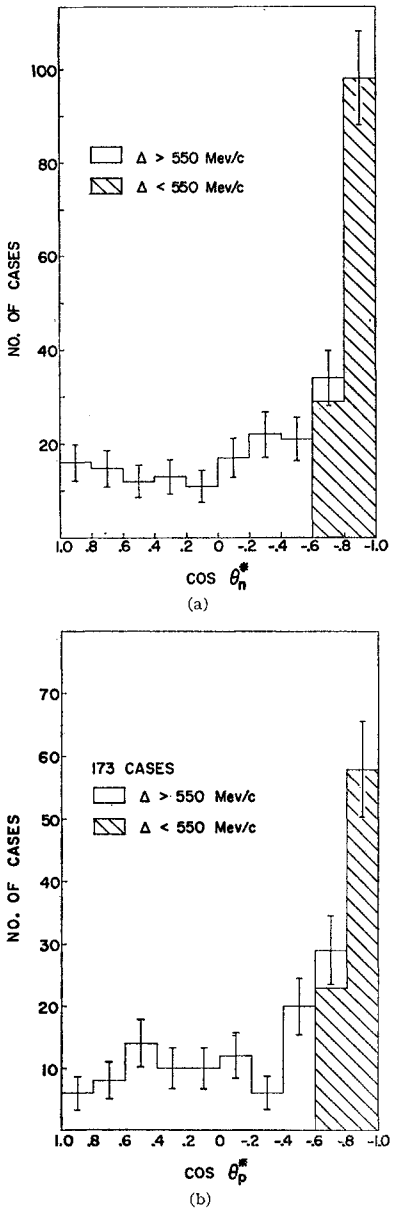

FIG. 10. Center-of-mass angular distributions, (a) for neutrons from $\pi^-+p\rightarrow\pi^-+\pi^++n$ events, and (b) for protons from $\pi^-+p\rightarrow\pi^-+\pi^0+p$ events. Cases with $\Delta<550$ Mev/c are indicated.

Since an extrapolation to the $\Delta^2=-\mu^2$ pole as suggested by Chew and Low[14] is not practical with the statistics available, the technique of Erwin *et al.*[16] has been used to estimate $\sigma_{\pi\pi}(\omega)$. Events with Δ less than some maximum are selected. For a low enough $\Delta_{\max}$, it is hoped that the equation of Chew and Low will provide an adequate description of the interaction and can be used to calculate values of $\sigma_{\pi\pi}(\omega)$ from the experimental data. The restriction to low momentum transfers should also help to eliminate cases of $T=J=\frac{3}{2}$ final-state pion-nucleon interactions. The procedure has the disadvantage that the $\pi-\pi$ cross section is determined off the energy shell, and, also, there is no way to estimate the effect of interfering matrix elements. In order to calculate $\sigma_{\pi\pi}(\omega)$, the events with $\Delta^2\leqslant\Delta_{\max}{}^2$ are separated into intervals of ω. The expression for $\partial^2\sigma/\partial\Delta^2\partial\omega^2$ is integrated over Δ^2, giving

$$\delta\sigma=\delta\omega\frac{\alpha f^2}{\pi\mu^2 q_{1L}{}^2}\omega^2(\tfrac{1}{4}\omega^2-\mu^2)^{\frac{1}{2}}\sigma_{\pi\pi}(\omega)\int_{\Delta_{\min}{}^2}^{\Delta_{\max}{}^2}\frac{\Delta^2 d\Delta^2}{(\Delta^2+\mu^2)^2},$$

where $\delta\sigma$ is determined experimentally for a given ω and all other factors except $\sigma_{\pi\pi}(\omega)$ can be calculated.

Erwin *et al.*[16] have combined their data from (π^-,π^+,n) and (π^-,π^0,p) events in order to obtain better statistics. This involved averaging the $\pi^-+\pi^0$ and $\pi^-+\pi^+$ cross sections, but these should be equal if a $T=1$ state is dominant. In this experiment, also, it appears that a

TABLE VIII. Four-momentum transfer distribution of events.

Interaction	All Δ	$\Delta<400$ Mev/c	$\Delta<550$ Mev/c	$\Delta>550$ Mev/c
$\pi^-+p\rightarrow\pi^-+\pi^++n$	259	68	127	132
$\pi^-+p\rightarrow\pi^-+\pi^0+p$	173	49	81	92

$T=1$ state must dominate, but since the results for (π^-,π^+,n) and (π^-,π^0,p) events appear slightly different they will be presented separately.

Evidence for a $T=1$ state at this energy is summarized in Table VII. Experimental cross sections for different processes are listed along with relative probabilities calculated for single dominant $\pi-\pi$ states of different isotopic spins.

The large π^+-p cross sections seem to imply the importance of some other enhancement, but the only $\pi-\pi$ state which is consistent with the π^--p experimental ratios is $T=1$.

In order to determine values of $\sigma_{\pi\pi}(\omega)$ by the method chosen, it is necessary to select events with Δ less than some $\Delta_{\max}$. The choice of $\Delta_{\max}$ involves a compromise. The value of $\Delta_{\max}$ should be as small as possible to eliminate most rescattering events and to insure that the formula to be used is a good approximation but must be large enough to allow acceptance of a reasonable number of events. Analysis has been carried out for two choices of $\Delta_{\max}$—550 Mev/c and 400 Mev/c corresponding to nucleon kinetic energies of 161 Mev and 85 Mev, respectively. The choice of 550 Mev/c allows acceptance of approximately half of all the events but appears to result in the inclusion of a number of cases involving $\pi-N$ final-state interactions. The choice of 400 Mev/c reduces the number of events by almost a factor of two.

In order to see the effects of a given choice of $\Delta_{\max}$, the c.m. distributions of angles and momenta for the secondary particles were examined for different ranges of Δ. The numbers of events involved in each region are listed in Table VIII.

Selection of low four-momentum transfers results in the selection of events in the backward peaks of the nucleon angular distributions as can be seen in Fig. 10. Angular distributions for the secondary pions are shown in Figs. 11 and 12. The effect of the selection procedure on the pion distributions cannot be predicted with the

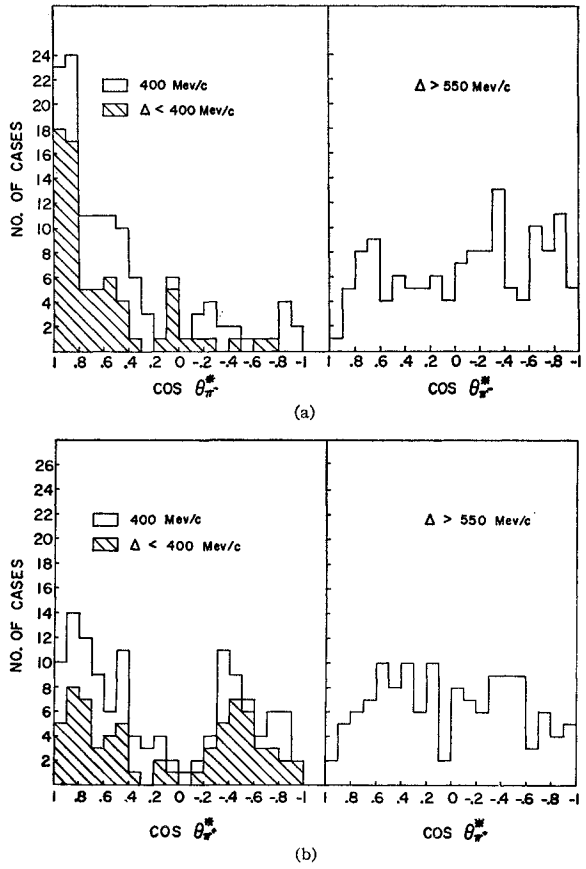

FIG. 11. Center-of-mass angular distributions, (a) for π^-, and (b) for π^+ from $\pi^-+p\rightarrow\pi^-+\pi^++n$. Events with $\Delta>550$ Mev/c and $\Delta<550$ Mev/c are shown separately. Events with $\Delta<400$ Mev/c are indicated.

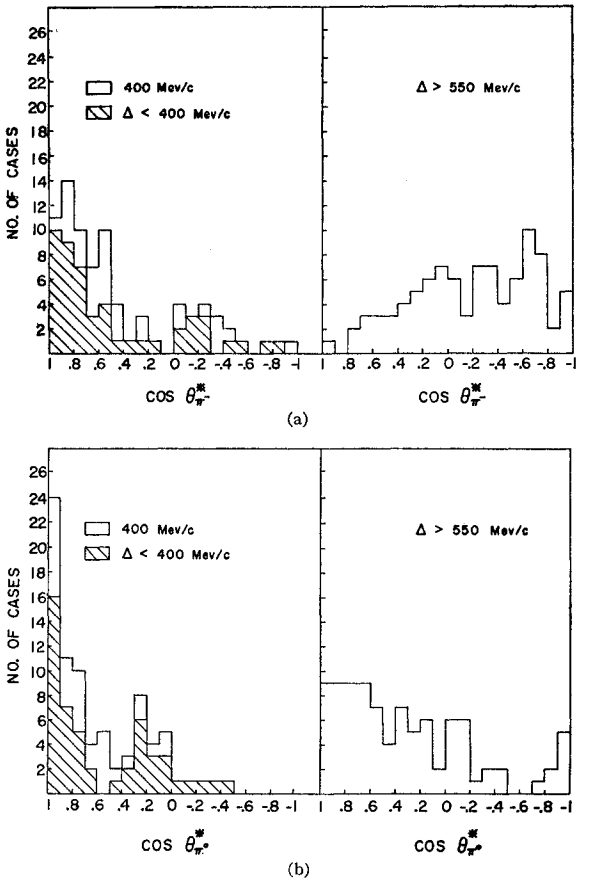

FIG. 12. Center-of-mass angular distributions, (a) and π^-, and (b) for π^0 from $\pi^-+p\rightarrow\pi^-+\pi^0+p$. Events with $\Delta>550$ Mev/c and $\Delta<550$ Mev/c are shown separately. Events with $\Delta<400$ Mev/c are indicated.

same precision. Qualitatively, one would expect that selection of backward nucleons would result in selecting forward pions. This is indeed the case, as can be seen from the distributions, except for the π^+ from (π^-,π^+,n) events. For high momentum transfers the distributions are more nearly isotropic.

Definite differences in c.m. momentum spectra for different intervals of Δ are also observed. The differences seem to be those which might be expected if a pion-pion interaction is important and if final-state pion-nucleon interactions occur in a large number of cases with large Δ. The momentum distributions are shown in Figs. 13 and 14. Again some difference between the (π^-,π^+,n) and (π^-,π^0,p) events are observed. In general, the pion momentum spectra for $\Delta>550$ Mev/c show peaking in the region near 540 Mev corresponding to the energy for a $T=J=\frac{3}{2}$ resonance between the other pion and the nucleon. The spectra for $\Delta\leqslant 550$ Mev/c tend to show more peaking in this region than the spectra for $\Delta\leqslant 400$ Mev/c, probably indicating the presence of some events with rescattering in the larger interval. The nucleon momentum spectra for $\Delta\geqslant 550$ Mev/c appear quite similar to spectra predicted by the isobar or statistical models while the spectra for lower Δ peak at lower momenta, an effect which can be interpreted as due to a $\pi-\pi$ resonance. The π^- momentum spectrum for the (π^-,π^+,n) events shows a very pronounced high-momentum peak which may indicate some type of diffraction effect.[41]

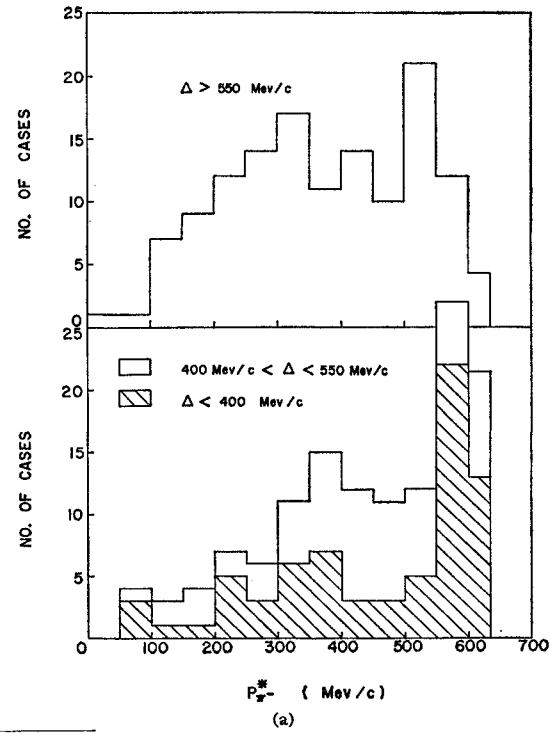

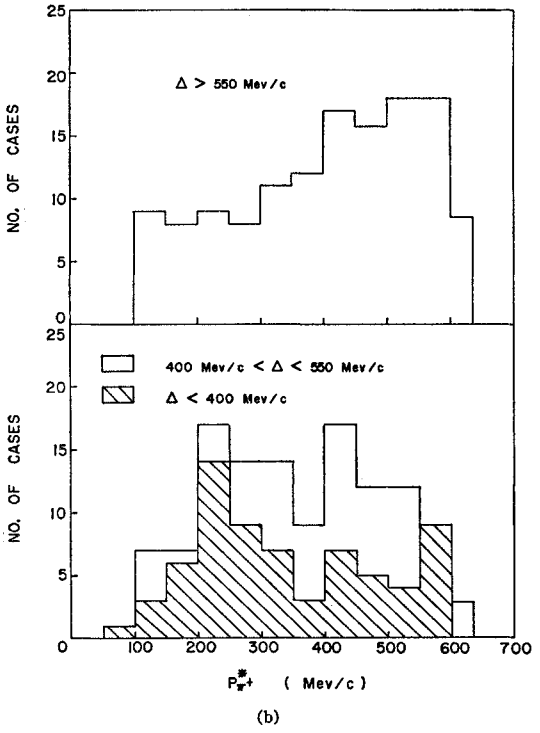

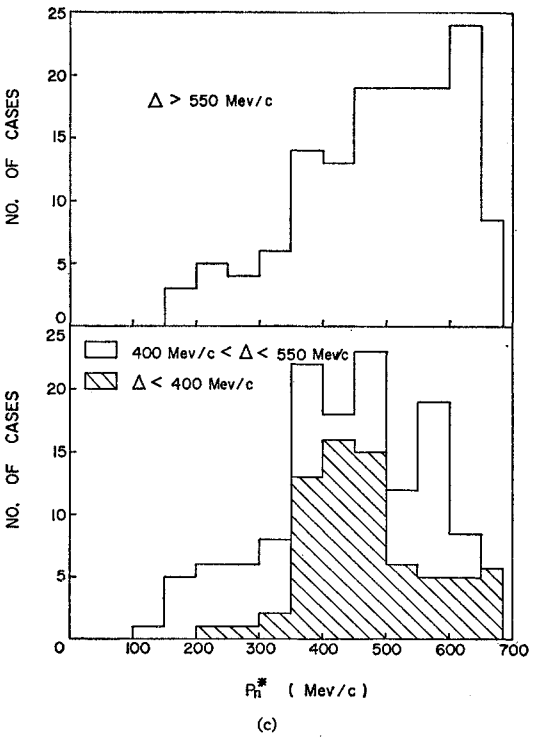

FIG. 13. Center-of-mass momentum distributions of secondary particles in $\pi^-+p\rightarrow\pi^-+\pi^++n$ events for different ranges of Δ. Distributions are shown, (a) for π^-, (b) for π^+, and (c) for n. Events with $\Delta>550$ Mev/c and $\Delta<550$ Mev/c are shown separately. Events with $\Delta<400$ Mev/c are indicated.

[41] M. L. Good and W. D. Walker, Phys. Rev. 120, 1857 (1960).

Once a value for Δ_{max} has been selected, the data may be examined for evidence of a $\pi-\pi$ resonance by calculating $\sigma_{\pi\pi}(\omega)$. Any resonance of appreciable size should show up as a peak in the distribution for dipion mass, ω. Histograms are shown of the values for ω for different ranges of Δ in Figs. 15 and 16. There appears to be a larger proportion of events in the range from 700 to 800 Mev/c^2 as Δ_{max} is decreased. The effect seems clearer in the (π^-,π^+,n) case than in the (π^-,π^0,p) case. The (π^-,π^0,p) spectra seem to contain a larger proportion of events with low dipion mass.

For the energy of this experiment the kinematic factors in the equation would result in a maximum in the dipion mass spectrum between 700 and 800 Mev even with constant $\pi-\pi$ cross section. The statistical and isobar models also predict peaks in about the same energy region. These models, though, would not be expected to show the differences with Δ_{max} which are observed. By taking smaller and smaller values of Δ_{max} one enriches the sample in peripheral collisions for which the Goebel, Chew-Low calculations are valid. As a result of this enrichment the computed $\pi-\pi$ cross section increased. The calculated cross sections as a function of ω are shown in Figs. 17 and 18. The cross sections have been calculated from ideograms rather than from the histograms of Figs. 15 and 16. The ideograms were constructed by assigning an uncertainty of ± 25 Mev/c^2 to the value of ω for each event and by using the calculated value of ω as the center of the interval for the event. The use of ideograms tends to smooth out fluctuations, due to the choice of intervals.

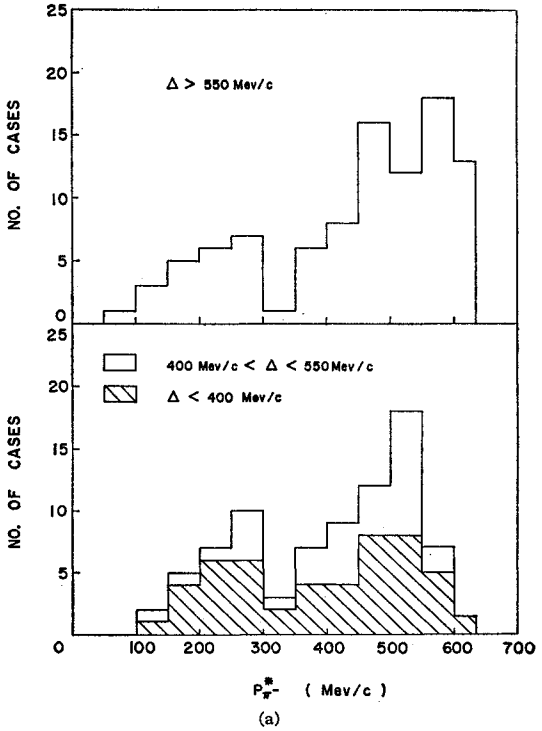

(a)

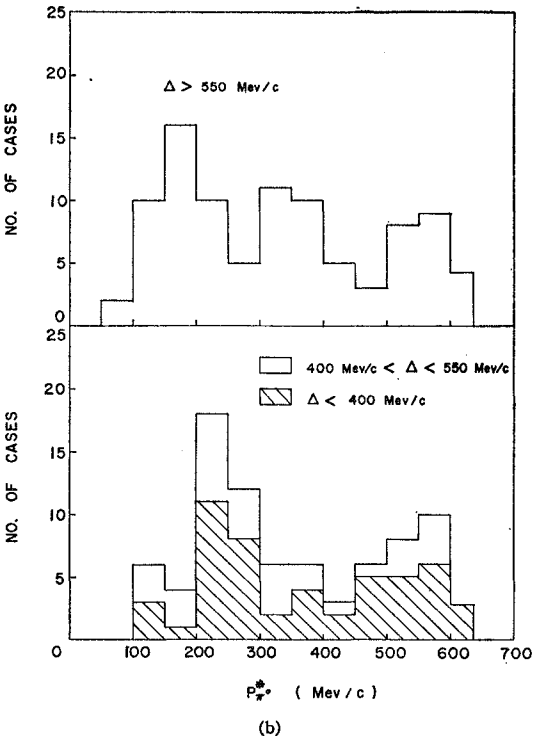

(b)

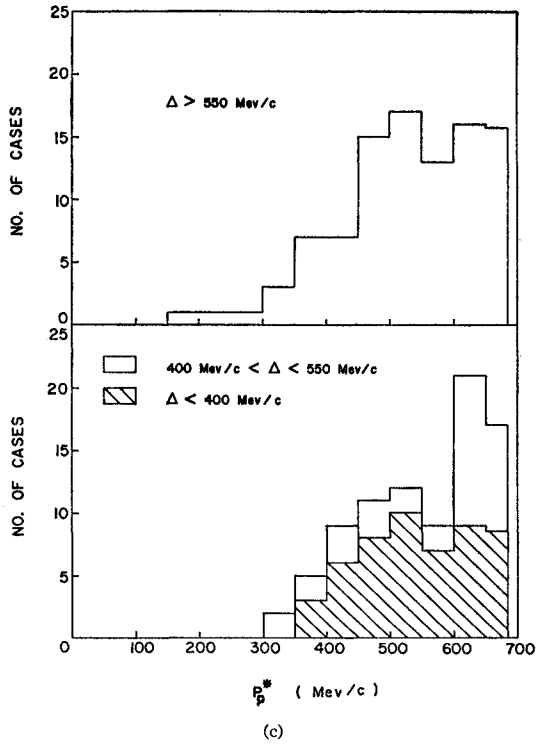

(c)

FIG. 14. Center-of-mass momentum distributions of secondary particles in $\pi^- + p \rightarrow \pi^- + \pi^0 + p$ events for different ranges of Δ. Distributions are shown, (a) for π^-, (b) for π^0, and (c) for p. Events with $\Delta > 550$ Mev/c and $\Delta < 550$ Mev/c are shown separately. Events with $\Delta < 400$ Mev/c are indicated.

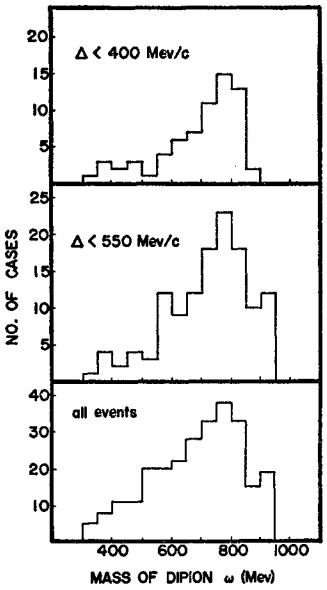

FIG. 15. Dipion mass distributions for $\pi^+ + p \rightarrow \pi^- + \pi^+ + n$ events. Distributions are shown for $\Delta < 400$ Mev/c, for $\Delta < 550$ Mev/c, and for all events.

The cross-section curves indicate the presence of a peak in $\sigma_{\pi\pi}(\omega)$ in the region from 700 to 800 Mev. The exact location of the peak cannot be determined with the limited statistics of this experiment, but the peak semms consistent with that found by Walker *et al.*[16] at 765 Mev. The maximum is about 60 to 70 mb for both reactions. This is slightly more than half the expected cross section ($12\pi\lambda^2 = 116$ mb) for a $T = J = 1$ resonance at 765 Mev. The peak appears more clearly in the (π^-,π^+,n) data than in the (π^-,π^0,p) data. No explanation for this is known. The height of the peak seems about the same in both cases. The difference seems to be due to additional events on both sides of the peak in the (π^-,π^0,p) case. The $\pi^- - \pi^0$ cross section seems higher at all energies below about 600 Mev.

Although the errors are larger for small ω both the $\pi^- - \pi^0$ and $\pi^- - \pi^+$ cross sections appear to rise at low energies. The low-energy rise for $\sigma_{\pi^- - \pi^+}$ could be explained by a low-energy $T = 0$ state. But this should not affect $\sigma_{\pi^- - \pi^0}$. A low-energy $T = 2$ state would be expected to affect both, but to have a greater effect on $\sigma_{\pi^- - \pi^0}$.

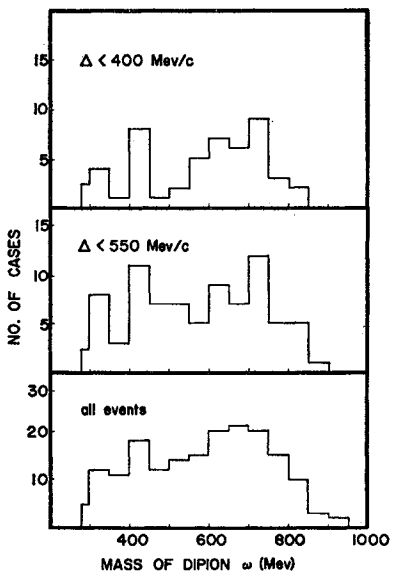

FIG. 16. Dipion distributions for $\pi^- + p \rightarrow \pi^- + \pi^0 + p$ events. Distributions are shown for $\Delta < 400$ Mev/c, for $\Delta < 550$ Mev/c, and for all events.

VII. CONCLUSIONS

The explanation of many features of the single pion production data from this experiment appears to be possible in terms of a pion-pion interaction which, in some cases, is followed by a final-state pion-nucleon interaction. The experimental values for the relative probabilities of different final states are consistent with a resonance in the $T = 1$ state of the pion-pion system as the dominant feature of pion production in this energy range. The position of the resonance appears to be in the neighborhood of 750-Mev total energy for the $\pi - \pi$ system. The data from this experiment are insufficient to determine the variation of $\sigma_{\pi\pi}$ with energy in any detail. A low-energy rise in $\sigma_{\pi\pi}$ appears to occur, but uncertainties are large in this region.

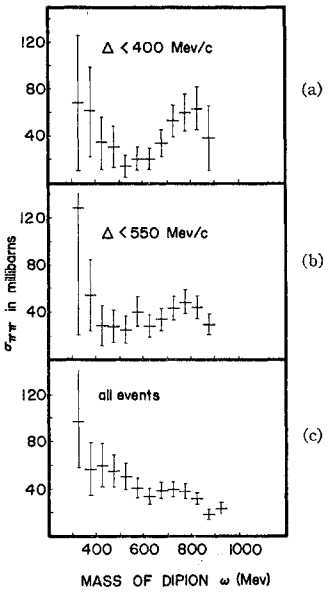

FIG. 17. Pion-pion interaction cross section for $\pi^- - \pi^+$ from $\pi^- + p \rightarrow \pi^- + \pi^+ + n$ events. The cross section has been calculated (a) from events with $\Delta < 400$ Mev/c, (b) from events with $\Delta < 550$ Mev/c, and (c) from all events.

The isobar model considered does not give quantitative agreement with the experiment. It seems certain however that some final-state interaction does occur in a sizeable fraction of the cases of single pion production. A more complete theory in which the $\pi - \pi$ interaction, the 3,3 isobar, and the symmetry of the $\pi - \pi$ system are considered has not been written, at least to the

authors' knowledge. Such a detailed theory would be a formidable task but would probably be quite rewarding.

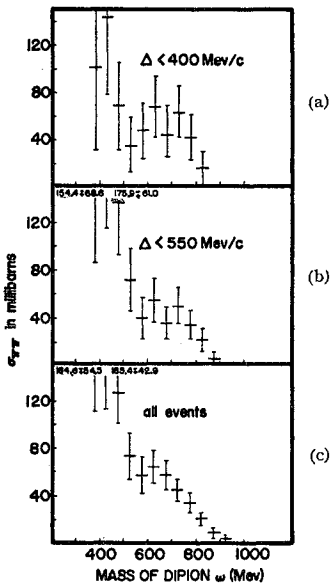

FIG. 18. Pion-pion interaction cross section for $\pi^- - \pi^0$ from $\pi^- + p \to \pi^- + \pi^0 + p$ events. The cross section has been calculated (a) from events with $\Delta < 400$ Mev/c, (b) from events with $\Delta < 550$ Mev/c, and (c) from all events.

VIII. ACKNOWLEDGMENTS

The pictures for this experiment were made available to us by Professor J. Steinberger and the Columbia Bubble Chamber Group. Their generosity is gratefully acknowledged. Dr. M. Schwartz and Dr. R. Plano kindly supplied details of the chamber and of the exposure.

Mrs. R. P. Chen did much of the scanning and measurement involved in the project.

Dr. R. M. Steinheimer kindly calculated the basic momentum spectra at 1.3 Bev for use in the analysis.

The help of the Numerical Analysis Laboratory at the University of Wisconsin and the Computing Center at the University of Kentucky in providing computing facilities and auxiliary equipment for the analysis was indispensible.

One of the authors (WDS) was aided by a National Science Foundation grant at the University of Kentucky during the latter stages of the work.

Helpful discussions with Dr. V. P. Kenney are acknowledged by WDS.

PHYSICAL REVIEW VOLUME 126, NUMBER 1 APRIL 1, 1962

Positive-Pion Cross Sections on Complex Nuclei*

JOHN C. CARIS,† EDWARD A. KNAPP,‡ VICTOR PEREZ-MENDEZ, AND WALTON A. PERKINS§
Lawrence Radiation Laboratory, University of California, Berkeley, California

(Received July 10, 1961)

Absorption and diffraction cross sections were measured for positive pions at a kinetic energy of 442 Mev. The target elements used were C, Al, Cu, and Cd. The absorption and diffraction cross sections were determined by fitting the experimental data (taken at six angles) to the shape given by the optical-model theory. The nuclear radius and the falloff parameter were taken to be approximately those determined from nuclear charge distribution measurements. The experimental data are compared with the results of the optical-model theory. Experimental values for the imaginary part of the potential V_I are in agreement with the theoretical value. However, the experimental values for the real potential V_R increase with increasing atomic number, becoming far larger than the theoretical value.

I. INTRODUCTION

MEASUREMENTS of total and absorption cross sections of pions in nuclei can be used to obtain information both on nuclear structure and on the pion-nucleon interactions. The theoretical interpretation of measurements of this sort is usually done using some form of an optical-model theory, as originally proposed by Fernbach, Serber, and Taylor[1] and since extended by many authors.[2,3]

Nuclear properties which can be deduced by experiments of this kind are the size and density distribution of nuclei. Analogous information on the charge distribution in nuclei has been obtained to a high degree of accuracy from the electron scattering experiments of

* This work was performed under auspices of the U. S. Atomic Energy Commission.

† Present address: Experimental Station, Polychemicals Department, E. I. du Pont de Nemours & Company, Wilmington, Delaware.

‡ Present address: Los Alamos Scientific Laboratory, University of California, Los Alamos, New Mexico.

§ Lawrence Radiation Laboratory, University of California, Livermore, California.

[1] S. Fernbach, R. Serber, and T. B. Taylor, Phys. Rev. **75**, 1352 (1949).

[2] K. M. Watson, Phys. Rev. **89**, 575 (1953); W. W. Wada, *ibid.* **92**, 152 (1953); N. C. Francis and K. M. Watson, *ibid.* **92**, 291 (1953); G. Takeda and K. M. Watson, *ibid.* **97**, 1336 (1955); L. S. Kisslinger, *ibid.* **98**, 768 (1955); R. M. Frank, J. L. Gammel, and K. M. Watson, *ibid.* **101**, 891 (1956); K. M. Watson, *ibid.* **105**, 1388 (1957).

[3] K. M. Watson and C. Zemach, Nuovo cimento **10**, 452 (1958).